

Cell-Type-Independent Expression of Inwardly Rectifying Potassium Currents in Mouse Fungiform Taste Bud Cells

Yoshiki NAKAO¹, Masahiro KOSHIMURA², Takashi YAMASAKI², Yoshitaka OHTUBO¹

¹Department of Human Intelligence Systems, Graduate School of Life Science and Systems Engineering, Kyushu Institute of Technology, Kitakyushu, Japan, ²Department of Chemical and Biological Engineering, National Institute of Technology (KOSEN), Sasebo College, Sasebo, Japan

Received September 27, 2019

Accepted February 25, 2020

Epub Ahead of Print May 29, 2020

Summary

Inwardly rectifying potassium (Kir) channels play key roles in functions, including maintaining the resting membrane potential and regulating the action potential duration in excitable cells. Using *in situ* whole-cell recordings, we investigated Kir currents in mouse fungiform taste bud cells (TBCs) and immunologically identified the cell types (type I-III) expressing these currents. We demonstrated that Kir currents occur in a cell-type-independent manner. The activation potentials we measured were -80 to -90 mV, and the magnitude of the currents increased as the membrane potentials decreased, irrespective of the cell types. The maximum current densities at -120 mV showed no significant differences among cell types ($p>0.05$, one-way ANOVA). The density of Kir currents was not correlated with the density of either transient inward currents or outwardly rectifying currents, although there was significant correlation between transient inward and outwardly rectifying current densities ($p<0.05$, test for no correlation). RT-PCR studies employing total RNA extracted from peeled lingual epithelia detected mRNAs for Kir1, Kir2, Kir4, Kir6, and Kir7 families. These findings indicate that TBCs express several types of Kir channels functionally, which may contribute to regulation of the resting membrane potential and signal transduction of taste.

Key words

Potassium • Membrane potentials • Signal transduction

Corresponding author

Y. Ohtubo, Department of Human Intelligence Systems, Graduate School of Life Science and Systems Engineering, Kyushu Institute of Technology, Hibikino 2-4, Kitakyushu-shi 808-0196, Japan.
E-mail: otsubo@brain.kyutech.ac.jp

Introduction

Taste buds detect taste substances in the oral cavity and transmit the information obtained to taste nerves (Podzimek *et al.* 2018). A typical taste bud contains 50-150 taste bud cells (TBCs), which are classified into four cell types on the basis of their morphology and functions: type I-IV (Murray 1973, Roper 2013). Type II TBCs express G protein-coupled taste receptors for sweet, bitter, and umami, and they secrete ATP as a transmitter to taste nerves through paracrine signaling (Adler *et al.* 2000, Chandrashekhar *et al.* 2000, Nelson *et al.* 2002, Nelson *et al.* 2001). Type III TBCs are sensitive to acid substances, and they release serotonin through synaptic vesicle-mediated signaling (Huang *et al.* 2008, Kataoka *et al.* 2008, Yoshida *et al.* 2009). Of close relevance to these functional differences among respective TBCs types is the fact that ion channels also express in a cell-type dependent manner: e.g. most outward rectifying currents in type II TBCs are insensitive to tetraethylammonium (TEA) and Cs⁺ ions, which are voltage-gated K⁺ channel blockers, whereas they are sensitive to TEA and Cs⁺ ions in type III TBCs (Kimura *et al.* 2014, Ohtubo *et al.* 2012). The channels insensitive to TEA and Cs⁺ ions are considered to be ATP-permeable channels. Recent studies have indicated that calcium homeostasis modulator 1 (CALHM1) and CALHM1/CALHM3 complex channels contribute to ATP secretion from type II TBCs (Kashio *et al.* 2019, Ma *et al.* 2017, Ma *et al.* 2018, Romanov *et al.* 2018). In addition, type III TBCs functionally and selectively

express voltage-gated Ca^{2+} channels for intracellular Ca^{2+} -dependent exocytosis (Clapp *et al.* 2006, DeFazio *et al.* 2006). Therefore, it is likely that clarifying the relationship between the cell type and the expression of ion channels will help elucidate the signal transduction mechanisms of taste.

Inwardly rectifying potassium (Kir) channels, through which more current is allowed to flow inward than outward, are expressed in a wide variety of tissue, including rodent TBCs (Kimura *et al.* 2014, Sun and Herness 1996). Kir channels are known to have diverse physiological functions depending on their type and their location. In TBCs, the Kir2.1 subtype functions as the acid-sensitive K^+ channel to mediate sour taste transduction (Ye *et al.* 2016). Moreover, TBCs express ATP-gated K^+ (K_{ATP}) channels that are co-expressed with glucose sensors on type 1 taste receptors 3 (T1r3)-positive taste cells to function as the T1r-independent sweet taste of sugar (Yee *et al.* 2011). However, little is known about the electrophysiological properties of Kir channels in each cell type.

In the present study, we showed that the membrane potential generating the Kir currents in our study was -80 to -90 mV, irrespective of cell types in the physiological conditions, that the current densities of Kir channels did not differ significantly between cell types, and that several types of Kir channel genes were expressed on the peeled lingual epithelia containing fungiform taste buds. We discuss the function of Kir channels in TBCs.

Methods

All experimental protocols were conducted in compliance with the Guiding Principles for the Care and Use of Animals in the Field of Physiological Sciences approved by the Council of the Physiological Society of Japan, and they were permitted by the Animal Institutional Review Board of Kyushu Institute of Technology, in accordance with the guidelines of the U.S. National Institutes of Health.

Preparation of peeled lingual epithelium

We peeled the lingual epithelium as described previously (Furue and Yoshii 1997, Furue and Yoshii 1998, Ohtubo *et al.* 2001). Forty ddY-strain male mice that were used for a general multipurpose model in Japan were purchased from Japan SLC (Hamamatsu, Japan). In brief, we sacrificed, by decapitation, 5-6-week-old

ddY-strain mice anesthetized with CO_2 , removed the tongue, hypodermically injected a collagenase solution into the tongue, and incubated the tongue at 25 °C for 3-4 min. We then used forceps under a stereomicroscope to peel off the epithelium containing fungiform papillae. Then, the peeled epithelia were mounted on a recording platform, with the basolateral membrane side of TBCs facing upward. The use of this preparation on the recording platform, allowed us to stably perform patch clamp recordings or optical recordings from TBCs over 1-2 h, as reported previously (Furue and Yoshii 1997, Furue and Yoshii 1998, Hayato *et al.* 2007, Ohtubo *et al.* 2001).

In situ whole-cell recordings

We used 24 mice to record voltage-gated currents using a conventional patch clamp method (Bebarova *et al.* 2015, Wen *et al.* 2017). Voltage-gated currents of fungiform TBCs were assessed under *in situ* whole-cell voltage-clamp conditions, as described previously (Furue and Yoshii 1997, Higure *et al.* 2003). In brief, the peeled epithelia containing TBCs that were mounted on the recording platform were placed under a microscope (BX50; Olympus corporation, Tokyo, Japan) with a 60× water-immersion objective. Recording electrodes were attached to the basolateral membranes of single TBCs. Under the voltage-clamp condition, voltage-gated currents were amplified and filtered at 10 kHz using a voltage-clamp amplifier (Axopatch 200B; Axon Instruments, CA, USA). Data were digitized using an A/D converter (Digidata 1322A; Axon Instruments) and were then stored using pCLAMP data acquisition and analysis software (ver. 9.0; Axon Instruments) on a personal computer. The recording electrode was filled with an intracellular KCl solution containing 2 mg/ml biocytin (Sigma-Aldrich, MO, USA) to identify cell types following immunohistostaining. The pipette resistance was approximately 5 MΩ in physiological saline.

Voltage-gated currents were generated with 40-ms test potentials of -120 to +80 mV in 5-mV steps every 1 s from a holding potential of -70 mV as a test pulse, unless noted otherwise. We attained a mean current of 38-40 ms at -120 mV by subtracting leak currents. The magnitude of the leak current at -120 mV was estimated by extrapolating the current-voltage relationships obtained between -70 and -50 mV. The membrane capacitance of TBCs was measured using pCLAMP data acquisition and analysis software. The magnitude of the maximal and mean currents (pA) through the ion

channels were divided by the membrane capacitance (pF) of their respective TBCs to obtain the current density (pA/pF). Further, we compared the current density thus obtained among the respective cell types.

Identification of cell types immunohistochemically

Following the patch clamp experiments, we stained the peeled epithelium with cell-type-specific antibodies to identify cell types of electrophysiologically recorded TBCs, as described previously (Kimura *et al.* 2014, Ohtubo *et al.* 2012). In brief, the peeled epithelia containing the biocytin-injected TBCs were fixed with 4% paraformaldehyde in phosphate-buffered saline (PBS), and they were then pre-treated with blocking solution containing 3% normal donkey serum, 0.3% Triton X, and 1% bovine serum albumin in PBS for 4 h at 25 °C. Lastly, immunostaining was carried out using primary antibodies dissolved in blocking solution for 24–48 h at 4 °C. After washing with PBS, the epithelia were incubated with Alexa Fluor-conjugated secondary antibodies and Alexa Fluor 633-conjugated streptavidin (1:100, S21375; Molecular Probe, CA, USA) for 24–48 h at 4 °C.

In this immunohistochemical experiment, we selected the cell-type markers IP₃R3 for type II cells and selected synaptosomal-associated protein 25 (SNAP-25) for type III cells in accordance with previous reports (Clapp *et al.* 2001, Ohtubo and Yoshii 2011, Yang *et al.* 2000). Anti-IP₃R3 mouse monoclonal antibody (1:50, BD-610312; BD Transduction Laboratories, KY, USA), and anti-SNAP-25 rabbit polyclonal antibody (1:1000, S9684; Sigma-Aldrich, MO, USA) were purchased from respective suppliers and used as primary antibodies. Alexa Fluor 488-conjugated donkey anti-rabbit IgG (1:400, A21206; Molecular Probe, OR, USA) and Alexa Fluor 555-conjugated donkey anti-mouse IgG (1:400, A31570; Molecular Probe, OR, USA) were used as secondary antibodies for primary antibodies of corresponding origin.

Immunostained epithelial preparations were viewed under a confocal microscope (TCS-SL; Leica Microsystems, Mannheim, Germany) as described previously (Ohtubo and Yoshii 2011). Confocal images were averaged from two or three images for each focal plane and were obtained over the entire length of the taste buds, with sequential acquisition in 1.5-μm steps and at optimal wavelengths for respective fluorescent dyes. Analysis of the averaged confocal images was performed using LAS AF Lite software (ver. 2.6.3; Leica

Microsystems) and Scion Image software (ver. β4.03; Scion Corporation, Frederick, MA, USA).

The soma of biocytin-injected TBCs were observed as fluorescent oval shapes and those of cell type markers as immunoreactive rings (Fig. 1D). In the overlay image, when either of the cell type markers surrounded the soma of a biocytin-injected TBC, we identified the TBC as either type II or III. When a biocytin-injected TBC was non-immunoreactive to both markers and contained apical portions, we identified the TBC as a type I cell.

Reverse transcription polymerase chain reaction (RT-PCR)

To screen for Kir channel gene expression, we performed reverse transcription polymerase chain reaction (RT-PCR) experiments, similar to our previous studies (Eguchi *et al.* 2008, Hayato *et al.* 2007, Mori *et al.* 2016). In brief, we immediately homogenized peeled lingual epithelia containing fungiform taste buds in ISOGEN (317-02503; NIPPON GENE, Tokyo, Japan) and extracted total RNA from the epithelia in ISOGEN according to the manufacturer's protocol. The extracted total RNA was incubated with DNase I solution (2270A; Takara Bio Inc., Siga, Japan) to remove any contaminating-genomic DNA. The cDNA synthesis and PCR were performed using QIAGEN One-Step RT-PCR kits (210212; QIAGEN, Hilden, Germany), unless noted otherwise. Total RNA (1 μl) was added to each premixed RT-PCR solution containing its own primer sets (Table 1). Reverse transcription was performed at 55 °C for 30 min. PCR cycles consisted of an initial step of 95 °C for 15 min and 40 subsequent cycles of 94 °C for 30 s (denaturation), 58 °C for 60 s (annealing), 72 °C for 90 s (extension), and a final extension step of 72 °C for 10 min with a thermal cycler (GeneAtlas; ASTEC Co., Ltd, Fukuoka, Japan). Amplicons were analyzed using 2% of agarose gel electrophoresis, stained with ethidium bromide, and visualized using UV illumination.

Specific primers for genes of TBC markers and Kir channels, apart from Kir6.2 (KCNJ11), were designed to span at least one intron by using Primr3Plus (web interface for primer design; <http://www.bioinformatics.nl/primer3plus>), as shown in Table 1. Using total RNAs extracted from brain, heart, and skeletal muscle, we confirmed that the designed primer sets, apart from Kir3.1 and Kir4.2, yielded a clear single band of the correct size. The primer set for Kir3.1 and Kir4.2 was designed to detect two isoforms. For the

Kir6.2 (KCNJ11) gene, which has a single exon, in each experiment, we conducted PCR without the RT reaction in parallel with RT-PCR to confirm contamination of genomic DNA. The experimental conditions for this PCR reaction were as follows: total RNA (1 µl) was added to premixed PCR solution (KOD-plus-; KOD-201, TOYOBO CO., LTD, Japan), and PCR cycles consisted of an initial step at 94 °C for 2 min, 40 subsequent cycles

at 94 °C for 30 s, 58 °C for 60 s, 68 °C for 60 s, and a final extension step at 68 °C for 10 min. We then confirmed that amplicons using primer sets for Kir6.2 yielded no clear single band without RT reaction. The housekeeping gene β-actin was used for positive control of peeled epithelium, brain, heart, and skeletal muscle. PLCβ2 and SNAP-25 were used for TBC markers as a positive control.

Table 1. Sequences of primer sets used for RT-PCR.

Gene (MGI symbol)	Forward primer 5' - 3'	Reverse primer 5' - 3'	Product size (bp)
<i>Kir1.1 (KCNJ1)</i>	CCTCAAAGAACGTCGGCCTTT	CCCTGATCAGCACTCTGCAC	110
<i>Kir2.1 (KCNJ2)</i>	CTTGCTTCGGCTCATTCTCT	AAGATGTCTGCCAGGTACCT	554
<i>Kir3.1 (KCNJ3)</i>	AAAAGCTGGAGCAAAAGCCG	GGGCCACCTCTTACCTTCC	519 (789)
<i>Kir2.3 (KCNJ4)</i>	GACCCTCCTCGGACCTTAC	AAGATGTCTGCCATGTAGCG	209
<i>Kir3.4 (KCNJ5)</i>	CTTATCAAGTCCCAGCAGAC	CTGGGAAGGTACTGGAGGAG	434
<i>Kir3.2 (KCNJ6)</i>	TTCCCCCTCAACCAGACTGAT	AGCTGAGCCTATAAGGAGGG	570
<i>Kir6.1 (KCNJ8)</i>	TGGCCACTAGCACCTCTATC	CCTGACATTGGTCACACAGA	719
<i>Kir3.3 (KCNJ9)</i>	TTTCTCGTCTCACCTCTCGT	CTTAGCTGTTCTCGGGAC	578
<i>Kir4.1 (KCNJ10)</i>	CCCGGACAAACCCATTATCTG	CACACCACACCAAAGAGGAA	411
<i>Kir6.2 (KCNJ11)</i>	ATAAGGCAGGCTTGTGAG	TGCCTGAAGTGCATTTGTA	258
<i>Kir2.2 (KCNJ12)</i>	TCCTTGTCTAGTTCAAGGCCA	ATGTTGCACTGACCGTTCTT	521
<i>Kir7.1 (KCNJ13)</i>	TCACAGCTGCATTCTCCTTC	AGAGTACAGCAGAGACACGA	309
<i>Kir2.4 (KCNJ14)</i>	GACCTGTTCACCATGTGT	CGATCAGTGCCTCCATCAAA	569
<i>Kir4.2 (KCNJ15)</i>	ATAGCAGAGCCCCATGGTAG	CACTCCTCTGTGATGGAACG	510 (522)
<i>Kir5.1 (KCNJ16)</i>	TAACCCTTGCAAGCTGAGAG	CATATGGCGCCACTTGGTAT	382
<i>β-actin (Actb)</i>	GTAAAGACCTCTATGCCAACAC	GTGTAAAACGCGAGCTCAGTAAC	289
<i>PLCβ2 (Plcb2)</i>	CTCGCTTGGGAAGTTGC	GCATTGACTGTCATCGGGT	226
<i>SNAP25 (Snap25)</i>	GGCAATAATCAGGATGGAGTAG	AAATTAAACCACTTCCCAGCA	310

Solutions

All solutions were prepared with deionized water and analytical grade reagents, which were purchased from Wako Pure Chemical Industries (Osaka, Japan), unless noted otherwise. The physiological saline solution contained 150 mM NaCl, 5 mM KCl, 2 mM CaCl₂, 0.5 mM MgCl₂, 10 mM glucose, and 5 mM HEPES-NaOH (pH 7.4; Sigma-Aldrich, MO, USA). The intracellular KCl solution contained 120 mM KCl, 2.4 mM CaCl₂, 5 mM MgCl₂, 10 mM EGTA (Dojindo Laboratories, Kumamoto, Japan), 30 mM KOH, 5 mM Na₂ATP, 0.3 mM Na₃GTP, 10 mM HEPES-KOH (pH 7.2; Sigma-Aldrich, MO, USA), and 2 mg/ml biocytin (Sigma-Aldrich, MO, USA). The collagenase solution consisted of 4 mg/ml collagenase type I

dissolved in physiological saline. PBS contained 137 mM NaCl, 8.1 mM Na₂HPO₄, 2.68 mM KCl, and 1.47 mM KH₂PO₄.

Statistics

Data of current densities obtained from the respective cell types (I-III) were analyzed using one-way ANOVA following Scheffe's multiple comparison test. Bartlett's test was used to determine whether the population showed equal variances among samples. A test for no correlation was used to determine the correlation between the current densities. The data are shown as means ± standard deviations (SDs), unless noted otherwise.

Results

Identification of cell types

To avoid misidentification, we injected biocytin into only one TBC in each lingual epithelium during the electrophysiological examinations. The injected biocytin diffused into the whole subcellular space of TBCs, including apical portions and the nuclei (Fig. 1). In contrast, the immunoreactive regions for IP₃R3 and SNAP-25 were observed as a ring surrounding the nucleus of TBCs. These confocal images were similar to those obtained in previous reports (Kimura *et al.* 2014, Ohtubo *et*

al. 2012). When either of the cell type markers surrounded the cell body of a biocytin-injected TBC, we identified the TBC as either type II or type III (Fig. 1). When a biocytin-injected TBC was non-immunoreactive to both markers and contained apical portions, we identified the TBC as a type I cell because type IV cells are oval and do not contain apical portions. We successfully injected biocytin into 24 TBCs, resulting in the identification of four type I, seven type II, and five type III cells following the electrophysiological recordings. The cell types of the eight remaining TBCs could not be identified because they were lost during the immunohistostaining processes.

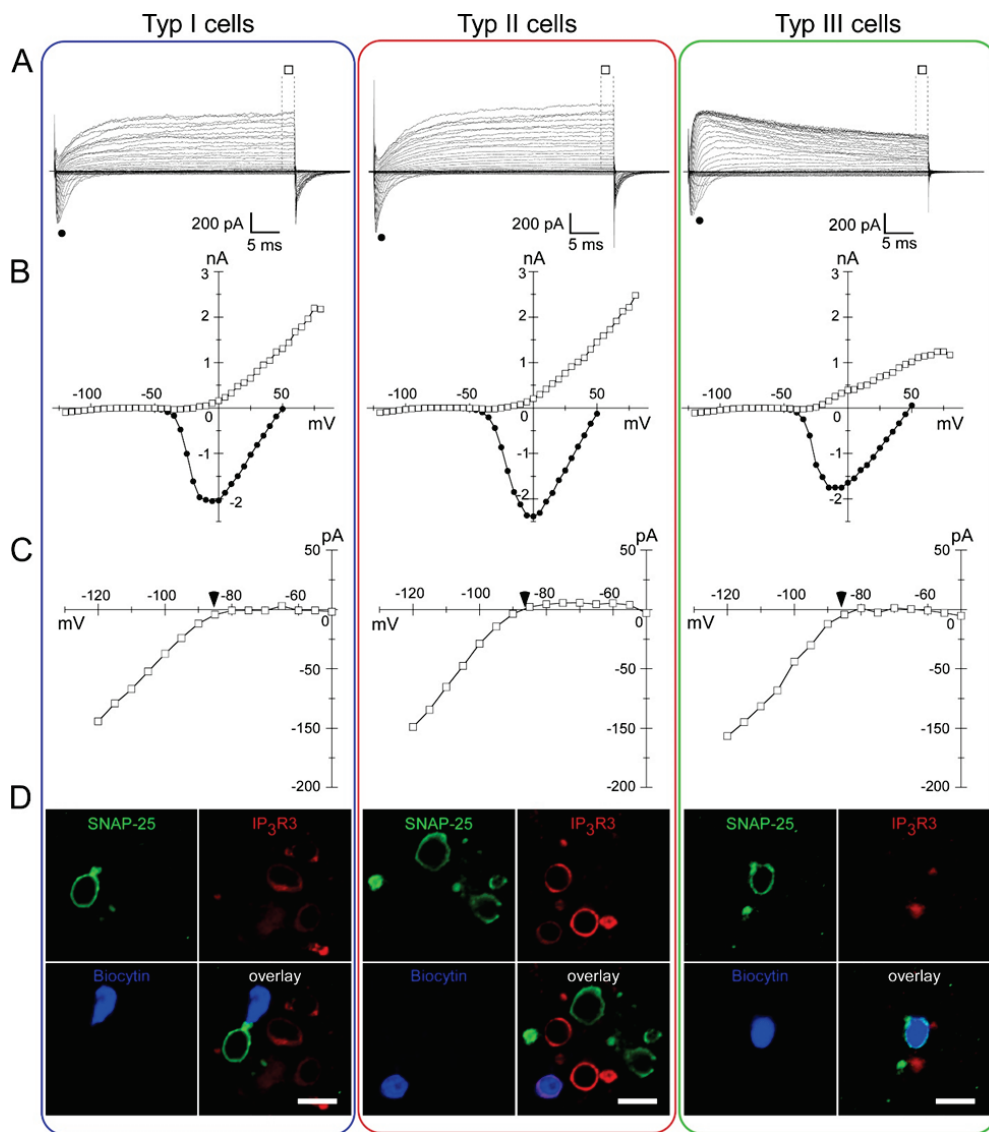


Fig. 1. Representative traces of voltage-gated currents obtained from a type I cell (non-immunoreactive cell, non-IRC), a type II cell (IP₃-IRC), and a type III cell (SNAP-25-IRC). Row (A): A family of voltage-gated currents obtained from the TBC. The currents are generated by test potentials from -120 to +80 mV in 5-mV increments from the holding potential of -70 mV. Row (B): Current-voltage (I-V) curves of respective TBCs, as shown in Row A. Symbols: peak transient inward current magnitude (closed circles) and averaged outwardly rectifying current magnitude (open squares), as shown in Row A. Row (C): Magnified I-V curves indicating the inwardly rectifying K⁺ currents. Arrow heads indicate the equilibrium potentials of K⁺ ions under our experimental conditions. Row (D): Immunoreactivity of cell type markers (green; SNAP-25, red; IP₃R3) and biocytin-injected TBCs (blue), from which these currents were recorded. Scale bars, 10 μm.

Inward rectifying K⁺ currents

TBCs of each cell type generated inward rectifying K⁺ (Kir) currents, in addition to outwardly rectifying currents and transient inward currents (Fig. 1). The membrane potential generating the Kir currents was at -80 to -90 mV, irrespective of cell type, and the magnitudes of the currents increased almost linearly with decreasing membrane potentials. The mean membrane capacitances of respective cell types were 6.0 ± 0.3 pF (mean \pm S.D., n=4) in type I cells, 5.8 ± 1.0 pF (n=7) in type II cells, 5.9 ± 1.1 pF (n=5) in type III cells, which is consistent with previous studies on the membrane capacitance of TBCs (Iwamoto *et al.* 2020, Kimura *et al.* 2014). There were no significant differences among the membrane capacitances of each cell type ($p > 0.05$, one-way ANOVA). The mean current densities, i.e. the mean currents in magnitude divided by membrane capacitance, of Kir currents were -20.9 ± 13.0 pA/pF (mean \pm S.D., n=4) in type I cells, -20.8 ± 15.6 pA/pF (n=7) in type II cells, and -19.3 ± 6.0 pA/pF (n=5) in type III cells at -120 mV (Fig. 2). Although variance in type I and type II cells tended to be larger than that in type III cells, there was homogeneity of variance ($p > 0.05$, Bartlett's test). There was no significant difference among cell types ($p > 0.05$, one-way ANOVA). These finding indicate that TBCs functionally express Kir channels with similar current density among cell types, although the current density appears to differ between individual cells.

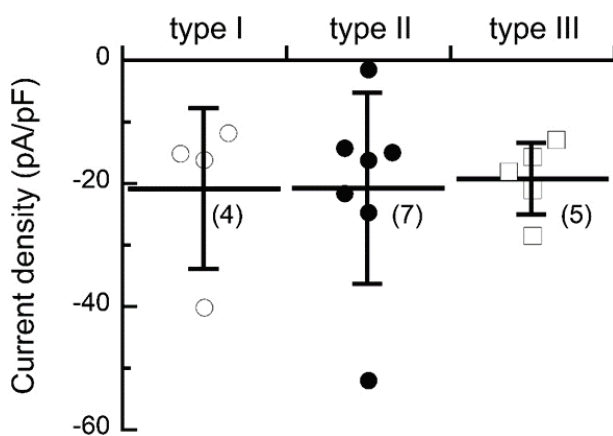


Fig. 2. Comparison of inwardly rectifying potassium current densities between cell types. Plotted data are current densities, i.e. current magnitude at -120 mV divided by the membrane capacitance of respective cells. Horizontal and vertical bars indicate means and SDs, respectively. There were no significant differences in the current densities between cell types ($p > 0.05$, one-way ANOVA). Numerals in parentheses indicate the number of TBCs examined.

To examine the relationship between the functional expression of Kir channels and of other voltage-gated channels, we compared the correlation of the current densities of ion channels (Fig. 3). There were no correlations either between the density of Kir currents and that of transient inward currents, or between the density of Kir currents and that of outwardly rectifying currents. Conversely, there was significant correlation between the density of transient inward currents and that of outwardly rectifying currents ($p < 0.05$, test for no correlation). According to previous pharmacological studies, the voltage-gated transient inward currents likely arise from the activation of voltage-gated Na⁺ channels (Furue and Yoshii 1997, Higure *et al.* 2003, Noguchi *et al.* 2003). Therefore, significant correlation between voltage-gated Na⁺ and outwardly rectifying currents facilitates the formation of action potentials.

RT-PCR

A total of 15 Kir subunit genes have been identified and classified into seven (Kir 1-7) subfamilies (Hibino *et al.* 2010, Reimann and Ashcroft 1999). To study the gene expression of these Kir subunits, we performed RT-PCR experiments using total RNA extracted from mouse peeled lingual epithelia containing fungiform taste buds. The results of RT-PCR revealed the expression of KCNJ1, KCNJ4, KCNJ10, KCNJ11, KCNJ12, KCNJ13, KCNJ14, and KCNJ15 (Fig. 4). Although KCNJ2 and KCNJ3 genes in the control experiments were detected by clear bands of the correct molecular size, those in the peeled lingual epithelia showed multiple bands. Thus, the expression of these two genes is unclear. The same results were obtained four times in independent experiments.

Discussion

In this study, the main finding is that all type I-III cells generate inwardly rectifying K⁺ (Kir) currents activated at -80 to -90 mV in our experimental condition. In addition, we have shown that the densities of the currents flowing Kir channels do not differ significantly between cell types. Therefore, it is likely that the functional significance of Kir channels may be in serving common roles, e.g. maintenance of the resting potentials, in addition to cell-type-specific roles, as contributions to sour and sugar taste transduction. To function in these various roles, TBCs express multiple types of genes for Kir channels, as indicated in both this study and previous studies (Ye *et al.* 2016, Yee *et al.* 2011).

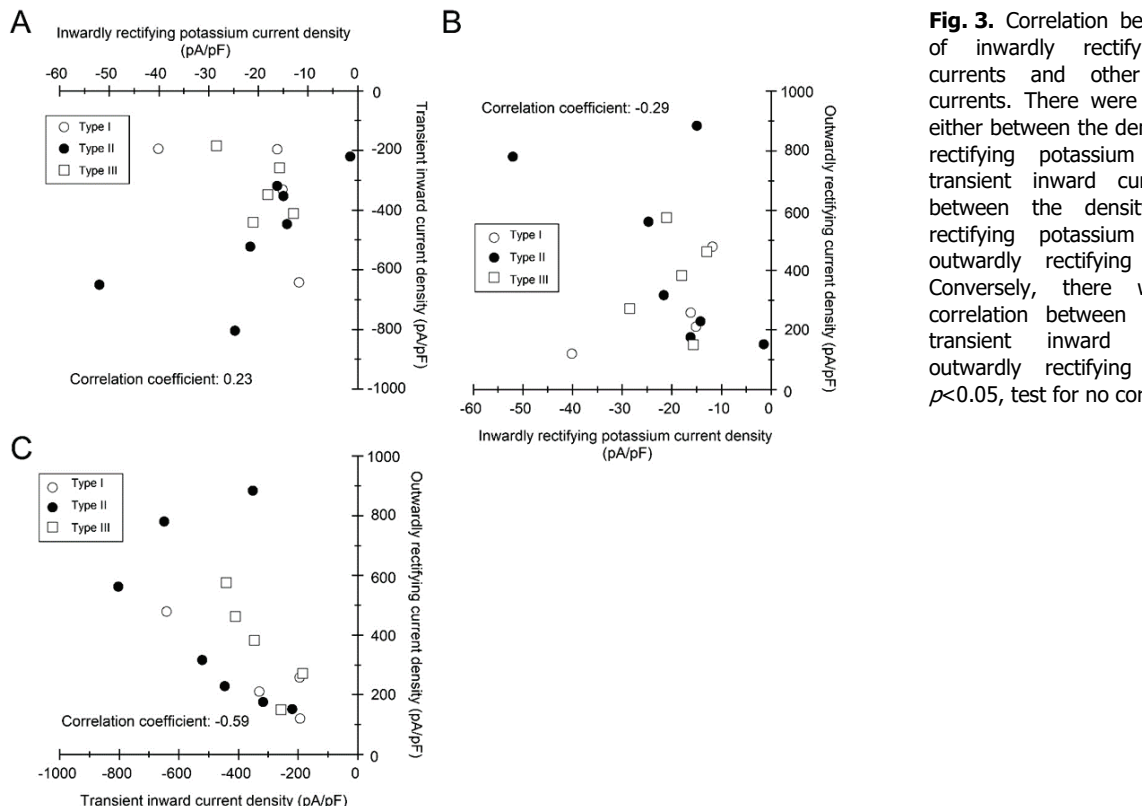


Fig. 3. Correlation between densities of inwardly rectifying potassium currents and other voltage-gated currents. There were no correlations either between the density of inwardly rectifying potassium currents and transient inward currents (**A**), or between the density of inwardly rectifying potassium currents and outwardly rectifying currents (**B**). Conversely, there was significant correlation between the density of transient inward currents and outwardly rectifying currents (**C**); $p<0.05$, test for no correlation).

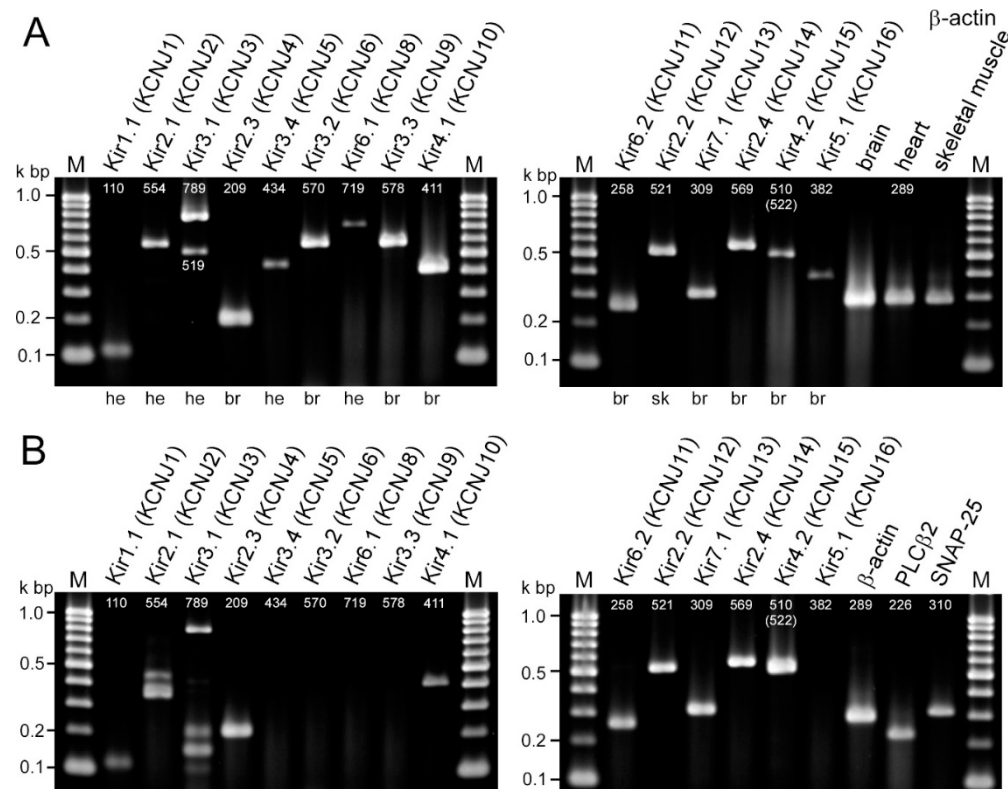


Fig. 4. Expression of Kir1, Kir2, Kir4, Kir6, and Kir7 mRNAs in peeled lingual epithelia. (**A**) Control studies with the primer sets used. Total RNAs were extracted from organs, such as mouse brains (br), hearts (he), and skeletal muscles (sk), in which the expression of respective Kir mRNAs was reported. Numerals in each line indicate expected product sizes. Examined primer sets, except for Kir3.1 and Kir4.2, yielded a clear single band with a correct size. The primer set for Kir3.1 and Kir4.2 was designed to detect two isoforms. (**B**) RT-PCR studies using total RNA extracted from peeled lingual epithelia containing fungiform taste buds detected the mRNAs of Kir1.1, Kir2.3, Kir4.1, Kir6.2, Kir2.2, Kir7.1, Kir2.4, and Kir4.2. Identical results were obtained in other RT-PCR experiments. Positive controls: β -actin, PLC β 2, and SNAP-25. M denotes molecular size markers.

In all cell types, the Kir current was generated at -80 to -90 mV, and it increased almost linearly with decreasing membrane potentials. The equilibrium potential (EK) of K⁺ ions was approximately -86 mV under our experimental conditions. As Kir channels are known to generate a large K⁺ conductance at membrane potentials negative to EK, our findings obtained from TBCs are consistent with this feature of Kir channels expressed in other tissues (Hibino *et al.* 2010).

The correlation coefficient between the density of Kir currents and transient inward currents was 0.23, and that between that of Kir currents and outwardly rectifying currents, which are non-correlated ($p>0.05$, test for no correlation), was -0.29. However, there was significant correlation between the density of transient inward currents and outwardly rectifying currents (-0.59; $p<0.05$, test for no correlation). Irrespective of cell types, the transient inward currents are voltage-gated Na⁺ currents based on electrophysiological and pharmacological relevant properties, as reported previously (Higure *et al.* 2003, Kimura *et al.* 2014, Ohtubo *et al.* 2012). Conversely, most of the outwardly rectifying currents in type III cells are voltage-gated K⁺ currents and those in type II cells are Cs⁺-insensitive currents, likely ATP-permeable currents (Kimura *et al.* 2014, Romanov *et al.* 2007). As both voltage-gated K⁺ and ATP-permeable currents contribute to the falling phase of action potentials, it stands to reason that there is significant correlation between the density of transient inward currents and that of outwardly rectifying currents.

Although the resting membrane potential of individual TBCs is unclear, the differences in the resting membrane potentials of individual type II cells may affect the taste signal transduction. Type II cells that detect

umami, bitter, and sweet substances secrete ATP to taste nerve endings as a predominant transmitter *via* membrane depolarization with action potentials. Because the equilibrium between closed and inactivated states of voltage-gated Na⁺ channels depends on the membrane potentials, the membrane potential just before receiving the taste substances may affect the ATP secretion. If a TBC has shallower resting membrane potentials, the number of inactivated Na⁺ channels increases. Hence, the action potential dependent-ATP secretion in this TBC may be decreased. In this study, we detected mRNAs for Kir6.2, although the Kir6.2-expressing cell types were unclear. Kir6.2 is a subunit of ATP-sensitive K⁺ channels (Hibino *et al.* 2010, Nichols 2006). It is possible that if some type II cells express Kir6.2 channels, individual type II cells may have different resting membrane potentials, as the intracellular concentration of ATP and ADP controls channel activity. These electrophysiological differences in individual type II cells might be important for taste signal transduction. Further experiments using a combination of patch clamp recording and single-cell RT-PCR are necessary to clarify the relationships between the resting membrane potentials of type II cells, the expression of Kir6.2 channels, and the signal transduction of taste.

Conflict of Interest

There is no conflict of interest.

Acknowledgements

This research was partially supported by Mr. Motoaki Miyoshi, the president of Miyoshi Rice Store, and by JSPS KAKENHI Grant-in-Aid for Scientific Research (C), Grant Number 15K07053.

References

- ADLER E, HOON MA, MUELLER KL, CHANDRASHEKAR J, RYBA NJ, ZUKER CS: A novel family of mammalian taste receptors. *Cell* 100: 693-702, 2000. [https://doi.org/10.1016/s0092-8674\(00\)80705-9](https://doi.org/10.1016/s0092-8674(00)80705-9)
- BEBAROVA M, MATEJOVIC P, SIMURDOVA M, SIMURDA J: Acetaldehyde at clinically relevant concentrations inhibits inward rectifier potassium current I(K1) in rat ventricular myocytes. *Physiol Res* 64: 939-943, 2015. <https://doi.org/10.1007/s00210-017-1341-z>
- CHANDRASHEKAR J, MUELLER KL, HOON MA, ADLER E, FENG L, GUO W, ZUKER CS, RYBA NJ: T2Rs function as bitter taste receptors. *Cell* 100: 703-711, 2000. [https://doi.org/10.1016/s0092-8674\(00\)80706-0](https://doi.org/10.1016/s0092-8674(00)80706-0)
- CLAPP TR, MEDLER KF, DAMAK S, MARGOLSKY RF, KINNAMON SC: Mouse taste cells with G protein-coupled taste receptors lack voltage-gated calcium channels and SNAP-25. *BMC Biol* 4: 7, 2006. <https://doi.org/10.1186/1741-7007-4-7>
- CLAPP TR, STONE LM, MARGOLSKY RF, KINNAMON SC: Immunocytochemical evidence for co-expression of Type III IP3 receptor with signaling components of bitter taste transduction. *BMC Neurosci* 2: 6, 2001. <https://doi.org/10.1186/1471-2202-2-6>

- DEFAZIO RA, DVORYANCHIKOV G, MARUYAMA Y, KIM JW, PEREIRA E, ROPER SD, CHAUDHARI N: Separate populations of receptor cells and presynaptic cells in mouse taste buds. *J Neurosci* 26: 3971-3980, 2006. <https://doi.org/10.1523/jneurosci.0515-06.2006>
- EGUCHI K, OHTUBO Y, YOSHII K: Functional expression of M3, a muscarinic acetylcholine receptor subtype, in taste bud cells of mouse fungiform papillae. *Chem Senses* 33: 47-55, 2008. <https://doi.org/10.1093/chemse/bjm065>
- FURUE H, YOSHII K: In situ tight-seal recordings of taste substance-elicited action currents and voltage-gated Ba currents from single taste bud cells in the peeled epithelium of mouse tongue. *Brain Res* 776: 133-139, 1997. [https://doi.org/10.1016/s0006-8993\(97\)00974-8](https://doi.org/10.1016/s0006-8993(97)00974-8)
- FURUE H, YOSHII K: A method for in-situ tight-seal recordings from single taste bud cells of mice. *J Neurosci Methods* 84: 109-114, 1998. [https://doi.org/10.1016/s0165-0270\(98\)00104-6](https://doi.org/10.1016/s0165-0270(98)00104-6)
- HAYATO R, OHTUBO Y, YOSHII K: Functional expression of ionotropic purinergic receptors on mouse taste bud cells. *J Physiol* 584: 473-488, 2007. <https://doi.org/10.1113/jphysiol.2007.138370>
- HIBINO H, INANOBE A, FURUTANI K, MURAKAMI S, FINDLAY I, KURACHI Y: Inwardly rectifying potassium channels: their structure, function, and physiological roles. *Physiol Rev* 90: 291-366, 2010. <https://doi.org/10.1152/physrev.00021.2009>
- HIGURE Y, KATAYAMA Y, TAKEUCHI K, OHTUBO Y, YOSHII K: Lucifer Yellow slows voltage-gated Na⁺ current inactivation in a light-dependent manner in mice. *J Physiol* 550: 159-167, 2003. <https://doi.org/10.1113/jphysiol.2003.040733>
- HUANG YA, MARUYAMA Y, STIMAC R, ROPER SD: Presynaptic (Type III) cells in mouse taste buds sense sour (acid) taste. *J Physiol* 586: 2903-2912, 2008. <https://doi.org/10.1113/jphysiol.2008.151233>
- IWAMOTO M, TAKASHIMA M, OHTUBO Y: A subset of taste receptor cells express biocytin-permeable channels activated by reducing extracellular Ca(2+) concentration. *Eur J Neurosci* 51: 1605-1623, 2020. <https://doi.org/10.1111/ejn.14672>
- KASHIO M, WEI-QI G, OHSAKI Y, KIDO MA, TARUNO A: CALHM1/CALHM3 channel is intrinsically sorted to the basolateral membrane of epithelial cells including taste cells. *Sci Rep* 9: 2681, 2019. <https://doi.org/10.1038/s41598-019-39593-5>
- KATAOKA S, YANG R, ISHIMARU Y, MATSUNAMI H, SÉVIGNY J, KINNAMON JC, FINGER TE: The candidate sour taste receptor, PKD2L1, is expressed by type III taste cells in the mouse. *Chem Senses* 33: 243-254, 2008. <https://doi.org/10.1093/chemse/bjm083>
- KIMURA K, OHTUBO Y, TATENO K, TAKEUCHI K, KUMAZAWA T, YOSHII K: Cell-type-dependent action potentials and voltage-gated currents in mouse fungiform taste buds. *Eur J Neurosci* 39: 24-34, 2014. <https://doi.org/10.1111/ejn.12388>
- MA Z, SAUNG WT, FOSKETT JK: Action potentials and ion conductances in wild-type and CALHM1-knockout type II taste cells. *J Neurophysiol* 117: 1865-1876, 2017. <https://doi.org/10.1152/jn.00835.2016>
- MA Z, TARUNO A, OHMOTO M, JYOTAKI M, LIM JC, MIYAZAKI H, NIISATO N, MARUNAKA Y, LEE RJ, HOFF H, PAYNE R, DEMURO A, PARKER I, MITCHELL CH, HENAO-MEJIA J, TANIS JE, MATSUMOTO I, TORDOFF MG, FOSKETT JK: CALHM3 is essential for rapid ion channel-mediated purinergic neurotransmission of GPCR-mediated tastes. *Neuron* 98: 547-561.e10, 2018. <https://doi.org/10.1016/j.neuron.2018.03.043>
- MORI Y, EGUCHI K, YOSHII K, OHTUBO Y: Selective expression of muscarinic acetylcholine receptor subtype M3 by mouse type III taste bud cells. *Pflugers Arch* 468: 2053-2059, 2016. <https://doi.org/10.1007/s00424-016-1879-5>
- MURRAY RG: The ultrastructure of taste buds In: *The Ultrastructure of Sensory Organs*. FRIEDMANN I (ed.), Amsterdam: North-Holland Publishing Company, 1973, pp 1-81.
- NELSON G, CHANDRASHEKAR J, HOON MA, FENG L, ZHAO G, RYBA NJP, ZUKER CS: An amino-acid taste receptor. *Nature* 416: 199-202, 2002. <https://doi.org/10.1038/nature726>
- NELSON G, HOON MA, CHANDRASHEKAR J, ZHANG Y, RYBA NJ, ZUKER CS: Mammalian sweet taste receptors. *Cell* 106: 381-390, 2001. [https://doi.org/10.1016/s0092-8674\(01\)00451-2](https://doi.org/10.1016/s0092-8674(01)00451-2)

- NICHOLS CG: KATP channels as molecular sensors of cellular metabolism. *Nature* 440: 470-476, 2006. <https://doi.org/10.1038/nature04711>
- NOGUCHI T, IKEDA Y, MIYAJIMA M, YOSHII K: Voltage-gated channels involved in taste responses and characterizing taste bud cells in mouse soft palates. *Brain Res* 982: 241-259, 2003. [https://doi.org/10.1016/s0006-8993\(03\)03013-0](https://doi.org/10.1016/s0006-8993(03)03013-0)
- OHTUBO Y, IWAMOTO M, YOSHII K: Subtype-dependent postnatal development of taste receptor cells in mouse fungiform taste buds. *Eur J Neurosci* 35: 1661-1671, 2012. <https://doi.org/10.1111/j.1460-9568.2012.08068.x>
- OHTUBO Y, SUEMITSU T, SHIOBARA S, MATSUMOTO T, KUMAZAWA T, YOSHII KY: Optical recordings of taste responses from fungiform papillae of mouse in situ. *J Physiol* 530: 287-293, 2001. <https://doi.org/10.1111/j.1469-7793.2001.02871.x>
- OHTUBO Y, YOSHII K: Quantitative analysis of taste bud cell numbers in fungiform and soft palate taste buds of mice. *Brain Res* 1367: 13-21, 2011. <https://doi.org/10.1016/j.brainres.2010.10.060>
- PODZIMEK S, DUSKOVA M, BROUKAL Z, RACZ B, STARAKA L, DUSKOVA J: The evolution of taste and perinatal programming of taste preferences. *Physiol Res* 67 (Suppl 3): S421-S429, 2018. <https://doi.org/10.33549/physiolres.934026>
- REIMANN F, ASHCROFT FM: Inwardly rectifying potassium channels. *Curr Opin Cell Biol* 11: 503-508, 1999. [https://doi.org/10.1016/s0955-0674\(99\)80073-8](https://doi.org/10.1016/s0955-0674(99)80073-8)
- ROMANOV RA, LASHER RS, HIGH B, SAVIDGE LE, LAWSON A, ROGACHEVSKAJA OA, ZHAO H, ROGACHEVSKY VV, BYSTROVA MF, CHURBANOV GD, ADAMEYKO I, HARKANY T, YANG R, KIDD GJ, MARAMBAUD P, KINNAMON JC, KOLESNIKOV SV, FINGER TE: Chemical synapses without synaptic vesicles: Purinergic neurotransmission through a CALHM1 channel-mitochondrial signaling complex. *Sci Signal* 11: 529, 2018. <https://doi.org/10.1126/scisignal.aao1815>
- ROMANOV RA, ROGACHEVSKAJA OA, BYSTROVA MF, JIANG P, MARGOLSKEE RF, KOLESNIKOV SS: Afferent neurotransmission mediated by hemichannels in mammalian taste cells. *EMBO J* 26: 657-667, 2007. <https://doi.org/10.1038/sj.emboj.7601526>
- ROPER SD: Taste buds as peripheral chemosensory processors. *Semin Cell Dev Biol* 24: 71-79, 2013. <https://doi.org/10.1016/j.semcd.2012.12.002>
- SUN XD, HERNESS MS: Characterization of inwardly rectifying potassium currents from dissociated rat taste receptor cells. *Am J Physiol* 271: C1221-C1232, 1996. <https://doi.org/10.1152/ajpcell.1996.271.4.c1221>
- WEN RJ, HUANG D, ZHANG Y, LIU YW: Bis(3)-tacrine inhibits the sustained potassium current in cultured rat hippocampal neurons. *Physiol Res* 66: 539-544, 2017. <https://doi.org/10.33549/physiolres.933354>
- YANG R, CROWLEY HH, ROCK ME, KINNAMON JC: Taste cells with synapses in rat circumvallate papillae display SNAP-25-like immunoreactivity. *J Comp Neurol* 424: 205-215, 2000. [https://doi.org/10.1002/1096-9861\(20000821\)424:2<205::aid-cne2>3.0.co;2-f](https://doi.org/10.1002/1096-9861(20000821)424:2<205::aid-cne2>3.0.co;2-f)
- YE W, CHANG RB, BUSHMAN JD, TU YH, MULHALL EM, WILSON CE, COOPER AJ, CHICK WS, HILL-EUBANKS DC, NELSON MT, KINNAMON SC, LIMAN ER: The K⁺ channel KIR2.1 functions in tandem with proton influx to mediate sour taste transduction. *Proc Natl Acad Sci U S A* 113: E229-E238, 2016. <https://doi.org/10.1073/pnas.1514282112>
- YEE KK, SUKUMARAN SK, KOTHA R, GILBERTSON TA, MARGOLSKEE RF: Glucose transporters and ATP-gated K⁺ (KATP) metabolic sensors are present in type 1 taste receptor 3 (T1r3)-expressing taste cells. *Proc Natl Acad Sci U S A* 108: 5431-5436, 2011. <https://doi.org/10.1073/pnas.1100495108>
- YOSHIDA R, MIYAUCHI A, YASUO T, JYOTAKI M, MURATA Y, YASUMATSU K, SHIGEMURA N, YANAGAWA Y, OBATA K, UENO H, MARGOLSKEE RF, NINOMIYA Y: Discrimination of taste qualities among mouse fungiform taste bud cells. *J Physiol* 587: 4425-4439, 2009. <https://doi.org/10.1113/jphysiol.2009.175075>